

Abstract

We report future projections of Surface Mass Balance (SMB) over the Greenland ice sheet (GrIS) obtained with the regional climate model MAR, forced by the outputs of three CMIP5 General Circulation Models (GCMs) when considering two different warming scenarios (RCP 4.5 and RCP 8.5). The GCMs selected in this study have been chosen according to their ability to simulate the current climate over Greenland. Our results indicate that in a warmer climate (i) the mass gained due to increased precipitation over GrIS does not compensate the mass lost through increased run-off; (ii) the surface melt increases non-linearly with rising temperatures due to the positive feedback between surface albedo and melt, associated with the expansion of bare ice zones which, in addition, decreases the ice sheet refreezing capacity; (iii) most of the precipitation is expected to fall as rainfall in summer, which further increases surface melt; (iv) no considerable change is expected on the length of the melting season, since heavier winter snowfall dampens the melt increase at the end of spring; (v) the increase of meltwater run-off versus temperature anomalies is dependent of the GCM-forced MAR ability to simulate the current climate; (vi) the MAR-simulated SMB changes can be approximated using the annual accumulated snowfall and summer 600 hPa temperature increase simulated by the forcing GCMs. In view of the large range in the CMIP5 future projections for the same future scenario, the GCM-based SMB approximations allow us to estimate what future projections are most likely within the CMIP5 multi-model ensemble. In 2100, the ensemble mean projects a sea level rise, resulting from a GrIS SMB decrease, estimated to be $+4 \pm 2$ cm and $+9 \pm 4$ cm for the RCP 4.5 and RCP 8.5 scenarios, respectively. The GrIS SMB should remain positive with respect to RCP 4.5 scenario and becomes negative around 2070 in the case of the RCP 8.5 scenario since a global warming $> +3^\circ\text{C}$ is needed. However, these future projections do not consider the positive melt-elevation feedback because the ice sheet topography is fixed through the whole simulation. In this regard, the MAR simulations suggest a cumulative ice sheet thinning by 2100 of $\sim 100\text{--}200$ m in the ablation zone. This highlights

Future projections of the Greenland ice sheet surface mass balance

X. Fettweis et al.

Title Page

Abstract

Introduction

Conclusions

References

Tables

Figures

⏪

⏩

◀

▶

Back

Close

Full Screen / Esc

Printer-friendly Version

Interactive Discussion



the importance of coupling climate models to an ice sheet model to consider the future response of both surface processes and ice-dynamic changes, and their mutual feedbacks to rising temperatures.

1 Introduction

The Surface Mass Balance (SMB) of the Greenland ice sheet (GrIS) can be approximated as the water mass gained by the winter snowfall accumulation minus the mass lost by the meltwater run-off in summer. The mass gain from rainfall as well as the mass loss from erosion from the net water fluxes (e.g., the sum of the evaporation, sublimation, deposition and condensation) and from the wind (blowing snow) appear to be negligible with respect to snowfall and water run-off (Box et al., 2004; Lenaerts et al., 2012).

A warmer climate will lead to an ice sheet surface thickening inland, due to increased solid precipitation, and a thinning along the GrIS periphery, due to increased surface melt. It is expected that the increase in meltwater run-off will only partly be compensated by the increase in snowfall in winter (Gregory and Huybrechts, 2006; IPCC, 2007; Fettweis et al., 2008; van Angelen et al., 2012; Rae et al., 2012), a phenomenon that has already been observed during last years of anomalously low SMB on the GrIS (van den Broeke et al., 2009; Tedesco et al., 2011; Rignot et al., 2011).

Beside impacting surface processes, increasing surface temperatures can also impact ice dynamics. Mass loss from ice calving is estimated to be of the same magnitude of the SMB, (Rignot et al., 2011), with recent mass loss being equally attributed to calving and SMB (van den Broeke et al., 2009). However, large uncertainties remain in the response of the GrIS dynamics to a surface melt increase (Zwally et al., 2002; Nick et al., 2009; Sundal et al., 2011) and, as currently observed (Rignot et al., 2011), the mass loss coming from an acceleration of the Greenland glacier flow in future should be less dominant compared with the SMB decrease at the time scale of this century. That is why, as a first step before evaluating the climate change impacts on the total

Future projections of the Greenland ice sheet surface mass balance

X. Fettweis et al.

Title Page

Abstract

Introduction

Conclusions

References

Tables

Figures

⏪

⏩

◀

▶

Back

Close

Full Screen / Esc

Printer-friendly Version

Interactive Discussion



ice sheet mass balance, we need to better quantify the projected GrIS SMB changes and more precisely the surface melt increase, which is the aim of this study.

Besides directly contributing to sea level rise, an increasing freshwater flux to the ocean from accelerated melting of the GrIS might affect the thermohaline circulation in the North Atlantic (Swingedouw et al., 2009). The contribution of the GrIS SMB decrease to the sea level rise from 2000 is currently evaluated to be 0–15 cm by 2100 (Gregory and Huybrechts, 2006; IPCC, 2007; Fettweis et al., 2008; Mernild et al., 2010; Vizcaino et al., 2010; Bengtsson et al., 2011; Franco et al., 2011). However, despite the GrIS melt importance for the global climate, large uncertainties remain in these estimations. One of the reasons for this is the fact that most of the current studies are based on the outputs of atmosphere-ocean General Circulation Models (GCMs), produced at a coarse horizontal spatial resolution (300 km). This limits their capabilities to capture SMB changes on the narrow ablation zone of the GrIS. Moreover, for reducing the computational load, the GCMs usually lack a realistic representation of the snow/firn/ice physics.

Regional atmospheric climate models (RCMs) are the ideal tools to understand the current Greenland ice sheet climate and to quantify its future change. The regional climate model MAR (for *Modèle Atmosphérique Régional*), fully coupled with a snow model and extensively validated to simulate the SMB of the Greenland ice sheet (Lefebvre et al., 2003, 2005; Fettweis, 2007; Fettweis et al., 2005, 2011b; Franco et al., 2012a), has been developed to study the Greenland climate and run at relatively high spatial resolution (25 km). Most of the works published in the literature concerning future projections of SMB over Greenland at high spatial resolution were carried out with models that do not account for the atmosphere-snow feedbacks occurring above the melt area, such as the positive feedback between surface albedo and melt (Mernild et al., 2008, 2010; Rae et al., 2012). These aspects are accounted for in the MAR model, which is here forced with outputs from several GCMs considering two scenarios of greenhouse gas emissions made for the next IPCC assessment report (AR5). This work fits into the ICE2SEA project (<http://www.ice2sea.eu>) of the 7th Framework

Future projections of the Greenland ice sheet surface mass balance

X. Fettweis et al.

Title Page

Abstract

Introduction

Conclusions

References

Tables

Figures



Back

Close

Full Screen / Esc

Printer-friendly Version

Interactive Discussion



Program (FP7), which aims to improve the projections of the land ice melt contribution to future sea level rise.

After a brief description of the MAR model in Sect. 2, Sect. 3 reports the results of the comparison of the MAR outputs obtained with ERA-INTERIM reanalysis forcing data over the period 1980–2011 with those obtained from MAR when forced by the selected GCMs for the overlapping period. In Sect. 4, we analyse future SMB projections, and in Sect. 5, we study the sensitivity of the SMB components to a fixed temperature anomaly independently of the forcing GCM and scenario used. Finally, future projections of GrIS SMB decrease based on 30 GCMs from the CMIP5 (Coupled Model Intercomparison Project Phase 5) database are presented in Sect. 6.

2 Data

2.1 The MAR model

The model used here is the regional climate model MAR coupled to the 1-D Surface Vegetation Atmosphere Transfer scheme SISVAT (Soil Ice Snow Vegetation Atmosphere Transfer) (Gallée and Schayes, 1994). The snow-ice part of SISVAT, based on the CEN (*Centre d'Etudes de la Neige*) snow model called CROCUS (Brun et al., 1992), is a one-dimensional multi-layered energy balance model that determines the exchanges between the sea ice, the ice sheet surface, the snow-covered tundra, and the atmosphere. It consists in a thermodynamic module, a water balance module taking into account the meltwater refreezing, a turbulence module, a snow metamorphism module, a snow/ice discretization module, and an integrated surface albedo module (Gallée et al., 2001). The blowing snow model, currently under development, is not used here. Since SISVAT is not coupled with an ice dynamics model, the same ice sheet mask and topography are used for simulating both current and future climates. This means that we do not take into account in our SMB projections the elevation feedbacks due to changes of the GrIS topography and mask.

Future projections of the Greenland ice sheet surface mass balance

X. Fettweis et al.

Title Page

Abstract

Introduction

Conclusions

References

Tables

Figures



Back

Close

Full Screen / Esc

Printer-friendly Version

Interactive Discussion



Weather Forecasts (ECMWF) are used to initialize the meteorological fields at the beginning of the MAR simulation in September 1957 and to force MAR every 6 h at its lateral boundaries. The Sea Surface Temperature (SST) and the Sea-Ice Cover (SIC) are also prescribed by the ECMWF reanalysis.

Due to a lack of SMB observations at the scale of the whole ice sheet, the ERA-INTERIM forced MAR (referenced as MARv2_{ERA-INTERIM} hereafter) simulation is used as the reference run in this manuscript, knowing that the SMB (Tedesco et al., 2011; Franco et al., 2012a), the (near-)surface temperature (Lefebvre et al., 2005; Fettweis et al., 2011b; Tedesco et al., 2012; Box et al., 2012), the downward shortwave radiation (Box et al., 2012), the melt extent (Fettweis et al., 2006, 2011b) and the albedo (Lefebvre et al., 2003; Fettweis et al., 2005) simulated by MAR have been successfully evaluated against in situ weather station data and satellite-derived data sets. In addition, according to Rae et al. (2012), MAR is among the best-performing RCMs, together with RACMO2 (van Angelen et al., 2012; Lenaerts et al., 2012). Some comparisons with RACMO2-based future projections will also be performed here for showing that some trends in our future projections are independent of the used RCM. As shown in Fig. S1 and Table S1 in the Supplement, MARv2 and RACMO2 forced by the ECMWF reanalyses compare well while they use different ice sheet masks and RACMO2 is run at a resolution of 11 km.

For computing future projections, we force MAR with 6 hly outputs (temperature, wind, humidity and surface pressure) from four GCMs (BCC-CSM1-1, CanESM2, NorESM1-M and MIROC5) of the CMIP5 database and from two GCMs (ECHAM5 and HadCM3) used by the FP7 ICE2SEA project (see Table 1). The version of ECHAM5 and HadCM3 is intermediate between the one used in the CMIP3 and CMIP5 data bases (Rae et al., 2012). As for the ECMWF-forced simulations, daily SST and SIC from GCMs are used to force the ocean surface conditions in SISVAT.

The two scenarios of future greenhouse gas (GHG) concentration increase used in this study, called RCP for Representative Concentration Pathways (Moss et al., 2010), are

Future projections of the Greenland ice sheet surface mass balance

X. Fettweis et al.

Title Page

Abstract

Introduction

Conclusions

References

Tables

Figures



Back

Close

Full Screen / Esc

Printer-friendly Version

Interactive Discussion

- RCP 4.5: mid-range scenario corresponding to a linear increase of radiative forcing towards $+4.5 \text{ w m}^{-2}$ towards 2080, and stabilizing afterwards. This scenario corresponds to an increase of the atmospheric greenhouse gas concentration during the 21st century to a level of $\sim 650 \text{ CO}_2$ equivalent p.p.m. by 2100.
- 5 – RCP 8.5: pessimistic scenario corresponding to a radiative forcing of $> +8.5 \text{ w m}^{-2}$ in 2100. This scenario corresponds to an increase of the atmospheric GHG concentration during the 21st century to a level of $> 1370 \text{ CO}_2$ equivalent p.p.m. by 2100.

As a comparison and for reader's convenience, results of RCP 6.0 ($\sim 850 \text{ CO}_2$ equivalent p.p.m. by 2100) and SRES A1B ($\sim 860 \text{ CO}_2$ equivalent p.p.m. by 2100) scenarios are also reported (see Table 1).

3 Evaluation over current climate

The aim of this section is to evaluate the ability of MAR forced by the different GCMs to simulate the present-day climate and SMB (1980–1999) over Greenland, in comparison to MARv2_{ERA-INTERIM}. Only the period 1980–1999 covered by ERA-INTERIM and used by the IPCC (2007) as the reference period over current climate is investigated here. However, knowing that the 1960's and 1970's are comparable to 1980–1999, a comparison over a longer period (e.g. 1970–1999) with MARv2_{ERA-40} does not impact the comparison, as shown in Figs. S1 and S2 in the Supplement. Finally, no comparison is made over the 2000's covered also by ERA-INTERIM because the last decade was considerably warmer than the previous ones.

A good representation of the current climate is a necessary but not the only condition to realistically simulate future climate changes. Indeed, a model that fails to reproduce the current climate generates projections that lack in reliability and validity since the response of the climate to a warming is not linear. That is particularly true for ice sheets, which are conditioned by the altitude of the 0°C isotherm. As we will see later, the

Future projections of the Greenland ice sheet surface mass balance

X. Fettweis et al.

Title Page

Abstract

Introduction

Conclusions

References

Tables

Figures



Back

Close

Full Screen / Esc

Printer-friendly Version

Interactive Discussion



Future projections of the Greenland ice sheet surface mass balance

X. Fettweis et al.

Title Page

Abstract

Introduction

Conclusions

References

Tables

Figures



Back

Close

Full Screen / Esc

Printer-friendly Version

Interactive Discussion



continent, deflecting to the northwest over Baffin Bay before reaching the western coast of Greenland, and generating a north-eastward circulation over Central Greenland. In Southern Greenland, the regional circulation is more influenced by northward circulation patterns. Biases at the RCM boundaries in the direction of the main flows impact the precipitation pattern.

The evaluation of the variables listed above is enough to explain most of the differences between MAR forced by the GCMs and MARv2_{ERA-INTERIM}. Biases in SST and SIC have indeed less impact on the MAR results (Hanna et al., 2009) and the specific humidity from GCMs compare generally well with the one from ERA-INTERIM (not shown here).

The CMIP5 GCMs used here (CanESM2, MIROC5 and NorESM1-M) have been selected among the most suitable GCMs from the CMIP5 database (with 6 hly outputs available at the model levels). They have also been selected by Belleflamme et al. (2012) for their ability to simulate the general circulation over Greenland at a daily time scale. Two RCM simulations using BCC-CSM1-1 and HadGEM2-ES as forcing are also shown to illustrate the impact of GCM-based temperature biases over current summer season on the simulation of the current SMB and its future projections by the RCMs. Indeed, while the HadGEM2-ES based general circulation compare very well with the reanalyses-based one (Belleflamme et al., 2012), its atmosphere is 1–2 °C too warm in summer while BCC-CSM1-1 is 2–3 °C too cold in summer. Finally, comparison with the ERA-40 reanalysis and the Reanalysis 1 of the National Centers for Environmental Prediction (NCEP) and the National Center for Atmospheric Research (NCAR) is also performed to evaluate the uncertainties within the reanalyses over Greenland, compared to the GCMs anomalies with respect to ERA-INTERIM.

3.1 Average annual rates and spatial variability of SMB components over 1980–1999

Table 2 lists the annual mean SMB components integrated over the whole ice sheet for the different simulations under current climate conditions (1980–1999). Figure 1 shows where SMB anomalies occur with respect to the $MARv2_{ERA-INTERIM}$ and Fig. 2 illustrates the differences among the different forcing models. Figures similar to Fig. 2 but for the 30 CMIP5 GCMs used in Section 6 are shown in the Supplement (see Fig. S3a, b).

With respect to the $MARv2_{ERA-INTERIM}$ simulation over 1980–1999, results show that:

- $MARv2/MARv1_{ERA-40}$ simulate less run-off and more precipitation because the ERA-40 atmosphere is a bit colder and drier than ERA-INTERIM. Part of these differences can be attributed to an improvement of the representation of the GrIS climate in ERA-INTERIM compared to ERA-40 (Dee et al., 2011; Screen and Simmonds, 2011). Moreover, these discrepancies (lower than the $MARv2_{ERA-INTERIM}$ inter-annual variability) give an estimation of the uncertainties made over current climate when MAR is forced by reanalyses.
- $MARv2_{BCC-CSM1-1}$ underestimates the snowfall along South-East Greenland because BCC-CSM1-1 underestimates the strength and the meridional component of the north-easterly flow that is characteristic to this area. Since the BCC-CSM1-1 atmosphere is statistically significantly colder ($2-3^{\circ}\text{C}$) than ERA-INTERIM in summer, $MARv2_{BCC-CSM1-1}$ underestimates the water run-off.
- $MARv2_{CanESM2}$ underestimates the SMB in the north-west of the Greenland ice sheet and overestimates it in the south and along the north-eastern coast. The SMB negative anomalies in the north-west are due to a combination of negative snowfall anomalies and positive water run-off anomalies induced by biases in summer temperature and winter accumulation as explained by Fettweis et al. (2011c). Indeed, beside directly impacting the mass gained, a lower winter

Future projections of the Greenland ice sheet surface mass balance

X. Fettweis et al.

Title Page

Abstract

Introduction

Conclusions

References

Tables

Figures

◀

▶

◀

▶

Back

Close

Full Screen / Esc

Printer-friendly Version

Interactive Discussion



accumulation is also responsible for a thinner snowpack above bare ice in the ablation zone, which induces premature bare ice exposure in summer, reducing the surface albedo and enhancing the surface melt (Mote, 2003; Tedesco et al., 2011). This snowfall negative anomaly is due to an underestimation by CanESM2 of the south-western flow, common in this area, impacting the amount of moisture that is advected to this area, while in the south of the ice sheet, the zonal flow is conversely overestimated by CanESM2 enhancing the precipitation amount in MAR. Finally, the pattern of $MARv2_{CanESM2}$ melt anomalies reflects the pattern of the CanESM2 JJA temperature biases at 700 hPa obtained in the case of ERA-INTERIM. At the scale of the whole ice sheet, these biases of opposite sign are compensated and $MARv2_{CanESM2}$ simulates annual SMB rate very close to $MARv2_{ERA-INTERIM}$.

- $MARv1_{ECHAM5}$ and $MARv1_{HadCM3}$ considerably underestimate the snowfall (mainly in the south) and overestimate the water run-off (mainly along the western and northern coast) because both forcing GCMs are too warm in summer (mainly HadCM3) and underestimate the strength of the large-scale atmospheric circulation (mainly ECHAM5) gauged here by the wind speed at 500 hPa. Similar to $MARv2_{CanESM2}$ in the north-west of the ice sheet, the accumulation underestimation induces a melt overestimation. Such biases impact the Equilibrium Line Altitude (ELA) that shifted 25–50 km towards the interior of the ice sheet with respect to $MARv2_{ERA-INTERIM}$. This explains why the SMB biases are the highest along the current ELA (plotted in red in Fig. 1).
- $MARv2_{MIROC5}$ best reproduces the spatial variability of SMB from $MARv2_{ERA-INTERIM}$ with biases similar to the discrepancies between $MARv2_{ERA-40}$ and $MARv2_{ERA-INTERIM}$. The highest biases occur in Southern Greenland where the MIROC5 atmosphere is 1 °C too cold in summer, which weakens the run-off in $MARv2$.

– $MARv2_{NorESM1-M}$ underestimates the run-off because NorESM1-M is $0-1^{\circ}\text{C}$ too cold in summer. The general circulation flow from NorESM1-M is generally too zonal in Southern Greenland (as BCC-CSM1-1), which explains why $MARv2_{NorESM1-M}$ overestimates the snowfall along the western coast and underestimates it along the eastern coast. At the scale of the whole ice sheet, the melt and snowfall biases add up and explain why $MARv2_{NorESM1-M}$ overestimates the average annual SMB rate by 100 GT yr^{-1} .

Finally, by comparing the outputs of MAR with those from RACMO2, both driven by ERA-INTERIM, we conclude that the inter-annual variability of SMB is higher than the mean differences between the two RCMs. Integrated over the whole ice sheet, the SMB rates from $RACMO2_{ERA-40}$ and $MARv2_{ERA-INTERIM}$ compare well over 1980–1999 (see Table 2 and Table S1 in the Supplement). In addition to the fact that RACMO2 is run at a spatial resolution of 11 km on a different ice sheet mask than MAR, differences in the physical schemes used in these two RCMs (Fettweis et al., 2011a) explain the small discrepancies between RACMO2 and $MARv2$ forced by ERA-INTERIM.

As HadGEM2-ES is one of the best CMIP5 GCM reproducing the general circulation from ERA-INTERIM but its atmosphere is too warm in summer, $RACMO2_{HadGEM2-ES}$ simulates successfully the precipitation amount but overestimates the melt by a factor of two with respect to both $RACMO2_{ERA-40}$ and $MARv2_{ERA-INTERIM}$. A more detailed evaluation of $RACMO2_{HadGEM2-ES}$ by comparison to $RACMO2_{ERA-INTERIM}$ is given in van Angelen et al. (2012).

3.2 Seasonal variability over 1980–1999

The simulations that best simulate the seasonality (i.e. an amplitude of $\sim 25^{\circ}\text{C}$ between summer and winter) of the near-surface temperature (TAS) are $MARv1_{ECHAM5}$, $MARv2_{MIROC5}$ and $MARv2_{NorESM1-M}$ with respect to $MARv2_{ERA-INTERIM}$ (see Fig. 3a). The $MARv2_{CanESM2}$ simulation is too cold in winter while $MARv1_{HadCM3}$ is too warm in summer and $MARv2_{BCC-CSM1-1}$ is too cold through the whole year. Finally, it should

Future projections of the Greenland ice sheet surface mass balance

X. Fettweis et al.

Title Page

Abstract

Introduction

Conclusions

References

Tables

Figures

◀

▶

◀

▶

Back

Close

Full Screen / Esc

Printer-friendly Version

Interactive Discussion

be noted that $MARv2_{ERA-40}$ is 0.25–0.5°C too cold every month with respect to $MARv2_{ERA-INTERIM}$, which gives an idea of the uncertainties in the reanalyses-forced MAR simulations.

On average, the MAR simulations that are too warm (resp. cold) in summer overestimate (resp. underestimate) the run-off (see Fig. 3b). However, $MARv1_{ECHAM5}$ overestimates the run-off while the TAS anomalies are lower than +0.5°C in summer. This is due to a relatively longer exposure of bare ice areas in summer resulting from the underestimation of snowfall (see Fig. 3c).

The $MARv2_{MIROC5}$ best simulates the seasonality of snowfall with a maximum in fall and a minimum in summer (only the anomalies are shown in Fig. 3c). The underestimation of snowfall by $MARv2_{BCC-CSM1-1}$ results from the underestimation of the general circulation dynamic by BCC-CSM1-1 and from the too low temperatures in winter, that prevents heavy precipitation events.

3.3 Inter-annual variability over 1980–2011

As shown by Fettweis et al. (2012), the JJA temperature at 600 hPa (T600) taken over an area covering Greenland ($70^\circ W \leq \text{longitude} \leq 20^\circ W$ and $60^\circ N \leq \text{latitude} \leq 85^\circ N$) can be used as a proxy of the surface melt variability simulated by MAR over current climate. The correlation of the MAR-based surface melt with the forcing-based TAS taken over the ice sheet is lower than T600 and the atmospheric temperatures taken at vertical levels (eg. 700 hPa) lower than 600 hPa are truncated by the ice sheet topography in most of the CMIP5 models. This explains why JJA T600 simulated by the forcing GCMs is plotted in Fig. 4.

From the 1960's to nearly the end of the 1990's, JJA T600 (and then the surface melt) was relatively stable over Greenland (Fettweis et al., 2012). Since summer 1998, ERA-INTERIM simulates a sharp increase of T600 and then a similar increase of the surface melt is simulated in both $MARv2_{ERA-INTERIM}$ and $RACMO2_{ERA-INTERIM}$ (see Fig. 5e). This warming is a combination of the Arctic amplified global warming (Serreze et al., 2009) and changes in the North Atlantic Oscillation (NAO) impacting the general

Future projections of the Greenland ice sheet surface mass balance

X. Fettweis et al.

Title Page

Abstract

Introduction

Conclusions

References

Tables

Figures



Back

Close

Full Screen / Esc

Printer-friendly Version

Interactive Discussion



Future projections of the Greenland ice sheet surface mass balance

X. Fettweis et al.

Title Page

Abstract

Introduction

Conclusions

References

Tables

Figures

⏪

⏩

◀

▶

Back

Close

Full Screen / Esc

Printer-friendly Version

Interactive Discussion



a snowfall decrease in the 2000's, as simulated by MARv2 and RACMO2 forced by ERA-INTERIM. With the RCP85, there is even a snowfall increase. This explains why MARv2_{CanESM2} underestimates the SMB decrease after 2005. It should also be noted that the MARv2_{CanESM2}-based SMB outputs compare very well in absolute values with the MARv2_{ERA-INTERIM}-based ones (Fig. 5a) over 1980–2004.

- MARv1_{ECHAM5} and MARv1_{HadCM3} underestimate the SMB through the whole observed period, as well as the current SMB decrease.
- MARv2_{MIROC5} and MARv2_{NorESM1-M} considerably overestimate the SMB after 2000 because they underestimate the current melt positive trend and do not simulate significant changes in snowfall in view of their inter-annual variability over 1980–1999.
- RACMO2_{HadGEM2-ES} works very well over 2000's by simulating the melt increase, the snowfall decrease and the RACMO2_{ERA-INTERIM} based SMB in absolute value. But, over the period 1980–1999, it simulates a significant snowfall increase and underestimates the SMB by a factor of two.

3.4 Conclusions on the evaluation

As mentioned by Franco et al. (2011) and by Belleflamme et al. (2012), no GCM is able to satisfactorily reproduce all behaviours of the current climate over GrIS and consequently, no GCM-forced RCM simulation can be selected as the best for making future projections. Indeed, MARv2_{BCC-CSM1-1} is too cold. While MARv2_{CanESM2} well reproduces the total ice sheet SMB and its inter-annual variability over the period 1980–2011, it underestimates the SMB at the north of the ice sheet and overestimates it at the south. The MARv1 simulations performed for the ICE2SEA project are impacted by several statistically significant biases and are hence likely less reliable. The MIROC5 and to a lesser extent NorESM1-M forced simulations reproduce well the SMB behaviour over the 1980–1999 period but they fail to simulate the SMB

decrease observed in the 2000's. Finally, RACMO2_{HadGEM2-ES} compares very well with the ERA-INTERIM forced simulations over 2000–2011 but fails to reproduce the 1980–1999 SMB behaviours.

Since the 2000's SMB decrease might be connected to the general circulation natural variability (not simulated by the GCMs) rather than to a long term change (see Fig. 4d), it is better to evaluate the performance of the RCM simulations over 1980–1999. In this case, MARv2_{CanESM2}, MARv2_{MIROC5} and MARv2_{NorESM1-M} are the best performers since most of the biases are statistically insignificant over the 1980–1999 period with respect to the MARv2_{ERA-INTERIM} inter-annual variability. The remaining simulations are used to see the impact of biases made over current climate (1980–1999) to their future projections with respect to the three previously cited reference simulations.

4 Future projections

4.1 Trends of the SMB components

Figure 5 and Table 3 indicate that the projected response of the GrIS SMB to the global warming is highly dependent on the GCM and scenario used for forcing MAR. Indeed, while all simulations agree in projecting an increase of snowfall and rainfall between +25 and +150 GT yr⁻¹ by 2100, the modelled changes in the water runoff vary between +200 and +1600 GT yr⁻¹ by 2100, with respect to the 1980–1999 mean. For the same RCP scenario, there is up to a factor of two between the melt increase simulated by MARv2_{CanESM2} and that simulated by MARv2_{NorESM1-M}. This is mostly due to the fact that there are several degrees of difference between the JJA T600 warming projected by CanESM2 and by NorESM1-M (see Fig. 4). Moreover, it should be noted that RACMO2_{HadGEM2-ES} (RCP45) projects SMB decrease by 2100 close to MARv2_{NorESM1-M} (RCP85) although there is a factor of two between the CO₂ concentrations by 2100 between both simulations and that future projections for ICE2SEA project using SRES A1B scenario (equivalent to the RCP60 scenario) are

Future projections of the Greenland ice sheet surface mass balance

X. Fettweis et al.

Title Page

Abstract

Introduction

Conclusions

References

Tables

Figures



Back

Close

Full Screen / Esc

Printer-friendly Version

Interactive Discussion



rather situated in the lower-range future projections for the RCP85 scenario. This is due to the GCMs sensitivity to a GHG concentration increase and to a melt overestimation over current climate, which amplifies the melt acceleration in future as discussed in Sect. 5.

At this stage, we can conclude that, for all models and all scenarios presented here, the mass gain due to increased snowfall is unable to compensate for the mass losses due to the increased run-off. This implies that the GrIS is projected to considerably lose mass from its surface and to contribute to the sea level rise (Fig. 5f), independently of the impact of increased run-off changes in the ice dynamics.

The absolute values of SMB (Fig. 5a) cannot be used to estimate when the SMB could become negative because, for the simulations underestimating the current SMB (e.g. RACMO2_{HadGEM2-ES}, MARv1_{HadCM3}), a negative SMB will occur earlier. But, if we use a SMB anomaly lower than -400 GT yr^{-1} as threshold for overcoming the biases made over current climate (Fig. 5b), the most pessimistic simulations do not project a negative 10-yr averaged SMB before the 2060's.

4.2 Spatial changes

All the simulations project a SMB increase of $\sim 100\text{--}200 \text{ mm WE yr}^{-1}$ in the current accumulation zone and a significant SMB decrease of $\sim 1000\text{--}3000 \text{ mm WE yr}^{-1}$ in the current ablation zone (see Fig. 6) for the period 2080–2099. The thinning rate of the ice sheet along its border and the shift of the ELA towards the centre of the ice sheet depend on the JJA warming amplitude shown in Fig. 6. The highest melt increase occur at the north of the ice sheet, because of the enhanced warming induced by the disappearance of the sea ice cover in the Arctic Ocean (Mernild et al., 2010; Franco et al., 2011). This decrease in the sea ice cover, apart from enhancing the atmospheric warming, also increases the water evaporation and therefore, explains why most of the simulations project a snowfall increase along the eastern margin. A thickening of the ice sheet is also projected near South-Dome (where the maximum of precipitation currently occurs). But, according to MARv2_{CanESM2} (RCP85), if the warming is too high,

Future projections of the Greenland ice sheet surface mass balance

X. Fettweis et al.

Title Page

Abstract

Introduction

Conclusions

References

Tables

Figures



Back

Close

Full Screen / Esc

Printer-friendly Version

Interactive Discussion



the snowfall increase is weakened because most of the precipitation falls as rainfall in summer and the mass gained by heavier snowfall is not enough for compensating the mass loss due to the water run-off increase. Finally, heavier snowfall could also occur in the north-east of the ice sheet but it is only simulated by MARv2_{NorESM1-M} and MARv2_{MIROC5}.

From Fig. 6, we also observe that the JJA TAS increase is not uniformly distributed over the ice sheet. Indeed, along the ice sheet margins, the current surface temperature (TS) is already close to 0 °C in JJA. Since the melting snow/ice TS is limited to the freezing point, this dampens the TAS increase. Nevertheless, in the north of the ice sheet and along the eastern coast, the TAS increase over tundra is generally higher over the neighbouring ice sheet. It is true that these pixels are the most affected by the disappearance of the sea ice cover in summer but these areas are currently covered by snow during a part of summer. With rising temperature, these areas could become snow free during most of the summer time and therefore a positive albedo feedback should also occur in these areas. Such effect is not as strong in the south-western tundra area because this area is already snow free in summer in the present-day climate.

4.3 Seasonal changes

The increase of temperature is not projected to occur uniformly through the year as shown in Fig. 3b. A first peak should occur in summer (August), likely due to the amplification of the albedo feedback mechanism, while a second peak is projected to occur in winter (January) when the impact of the sea ice decline is the highest over Greenland according to Deser et al. (2010).

According to our results, the seasonality of the SMB components should not change a lot in the future (see Fig. 3). The melting season should still be limited to the current melting season (from May to September), even for extreme scenarios, as the one obtained in the case of MARv2_{CanESM2} (RCP85) as shown by Franco et al. (2012b). The highest water run-off increase will occur in July and August but no considerable run-off increase is projected in May.

Future projections of the Greenland ice sheet surface mass balance

X. Fettweis et al.

Title Page

Abstract

Introduction

Conclusions

References

Tables

Figures



Back

Close

Full Screen / Esc

Printer-friendly Version

Interactive Discussion



GCM outputs only, we found the forcing GCM variables that best explain the changes in the SMB components simulated by the forced RCM. Since the multi-model mean is often considered by the IPCC as the best estimate of the simulated climate response to both natural and anthropogenic forcings, it is interesting to evaluate which GCM presented here is the closest to the CMIP5 ensemble mean.

5.1 Precipitation

With rising temperatures, a part of the precipitation currently falling in solid phase is projected to fall in liquid phase. We can see in Fig. 7a that the rainfall amount increases almost linearly with the GrIS TAS anomaly taken over JJA, when most of the rainfall events occur. The rainfall increase is similar for all simulations, with an exception of RACMO2_{HadGEM2-ES} which simulates a steeper increase. However, it should be noted that the rainfall increase does not contribute as a mass gain in the SMB equation in first approximation. Indeed, most of the rainfall events occurs over bare ice areas or liquid water saturated areas where liquid water runs off in both MAR and RACMO2 models. That is why, run-off minus rainfall (called meltwater run-off hereafter) will be discussed in the next section.

The sensitivity of the snowfall amount to a warmer climate is more simulation dependent than rainfall, although all simulations project a snowfall increase with rising temperatures. Indeed, in a warmer climate, there is more evaporation above the ocean and the atmosphere can contain more water vapour. This leads to higher moisture transport inland and, consequently, heavier precipitation. However, the part of precipitation that currently falls as snowfall is projected to fall as rainfall with rising temperatures, which dampens the snowfall increase vs temperature increase. However, it should be mentioned that total precipitation (snowfall + rainfall) increases agree well with the relative precipitation change estimated to be $5\% K^{-1}$ by Gregory and Huybrechts (2006) and plotted in black in Fig. 7b. A mean value of $700 GT yr^{-1}$ over current climate is used for plotting the $5\% K^{-1}$ relative precipitation change.

Future projections of the Greenland ice sheet surface mass balance

X. Fettweis et al.

Title Page

Abstract

Introduction

Conclusions

References

Tables

Figures

⏪

⏩

◀

▶

Back

Close

Full Screen / Esc

Printer-friendly Version

Interactive Discussion



Conversely to rainfall, the snowfall increase is not only driven by the rising temperatures. Indeed, to the snowfall increase in response of higher TAS is superposed the snowfall inter-annual variability ($\sim 50\text{--}70 \text{ GT yr}^{-1}$ over current climate) which is of the same order of magnitude as the snowfall increase. Since the snowfall inter-annual variability is driven by the GCM-based general circulation (Schuenemann and Cassano, 2010), the RCM-based annual snowfall anomaly can then be estimated using the annual snowfall from the GCM as shown in Fig. S4 in the Supplement. For estimating the snowfall over GrIS from GCMs, we select the GCM pixels located over the region covering the Greenland ($70^\circ \text{W}\text{--}20^\circ \text{W}$ and $60^\circ \text{N}\text{--}85^\circ \text{N}$) and having an altitude of at least 1000 m a.s.l using the orography (variable OROG in the CMIP5 data base) of each GCM. Since snowfall (variable PRSN) is given in $\text{kg m}^2 \text{ s}^{-1}$ in the CMIP5 database, we convert these values in GT yr^{-1} by using a constant factor $365 \cdot 24 \cdot 3600 \cdot k$, where k is a parameter fixed to 1.6 to achieve the best comparison of the GCM-based snowfall versus RCM-based snowfall.

5.2 Meltwater run-off and refreezing

According to Box et al. (2004) and Fettweis et al. (2008), the GrIS meltwater run-off variability can be approximated by the JJA GrIS TAS, as confirmed in Fig. 7c. In Fettweis et al. (2008), a linear relationship based on JJA TAS was used for estimating future meltwater run-off changes, considering that this relationship was only based on MAR results over current climate. However, for TAS higher than $2\text{--}3^\circ \text{C}$, both MAR and RACMO2 results show that the meltwater run-off rate non-linearly increases with rising JJA TAS as already pointed out by Fettweis et al. (2011c) and therefore, a second order polynomial equation is needed for better estimating the meltwater run-off increase with respect to TAS changes. As explained by Franco et al. (2012b), this non-linear meltwater run-off increase with rising temperatures can be interpreted as the consequence of the surface albedo positive feedback mechanism associated with the extension in summer of bare ice areas (with an albedo $\sim 20\%$ lower than the albedo of melting snow). This confirms the necessity of taking into account the bare ice zones in the models as

Future projections of the Greenland ice sheet surface mass balance

X. Fettweis et al.

Title Page

Abstract

Introduction

Conclusions

References

Tables

Figures

⏪

⏩

◀

▶

Back

Close

Full Screen / Esc

Printer-friendly Version

Interactive Discussion



highlighted by Rae et al. (2012). In addition, contrary to meltwater run-off, meltwater refreezing slightly increases in a linear fashion with rising JJA TAS (see Fig. 7c). This is because most of meltwater run-off increase occurs in the ablation zone, where ice lenses into the snowpack prevent efficient percolation and subsequent refreezing in the beginning of winter. Therefore, the refreezing capacity of the ice sheet is projected to decrease with the bare ice areas extension, which allows a non-linear increase of meltwater run-off (van Angelen et al., 2012).

Regarding the sensitivity of meltwater run-off to JJA TAS increase, it is function of the ability of the GCM-forced MAR to successfully represent the current run-off rate simulated by MARv2_{ERA-INTERIM}, since the response of melt is non-linearly dependent from rising temperatures. This means that the simulations that overestimate meltwater production in the current climate (MARv1_{ECHAM5}, MARv1_{HadCM3} and RACMO2_{HadGEM2-ES}) project a larger sensitivity than MARv2_{BCC-CSM1-1}, which is too cold in the current climate. The other simulations (MARv2_{CanESM2}, MARv2_{MIROC5}, MARv2_{NorESM1-M}), which better simulate the current melt rate, agree for giving intermediate sensitivities. However, the sensitivity is a bit lower for MARv2_{NorESM1-M} because it simulates the highest snowfall increase (including in summer) which impacts the melt in summer (Mote, 2003).

Anomaly values instead of absolute values are often used in future projections for masking biases over current climate. However, Fig. 7c shows that the meltwater run-off anomalies vs JJA TAS anomalies are different and depend upon the ability of simulating the current climate. This is particularly true over Greenland, where the SMB sensitivity will be different depending on if we are looking at areas above or below the current 0°C isotherm. However, the discrepancies between the meltwater run-off sensitivities to JJA TAS increase are lower than the projected changes.

The meltwater run-off anomalies cannot be derived from JJA TAS anomalies over GrIS from GCMs as from RCMs. Indeed, as shown in Fig. S5 from the Supplement, JJA TAS anomalies from RCM vs the ones from the forcing GCM are dependent on the GCM and its physical schemes. Depending on the forcing GCM, the GCM

Future projections of the Greenland ice sheet surface mass balance

X. Fettweis et al.

Title Page

Abstract

Introduction

Conclusions

References

Tables

Figures

⏪

⏩

◀

▶

Back

Close

Full Screen / Esc

Printer-friendly Version

Interactive Discussion

underestimates or overestimates the JJA TAS changes simulated by the forced RCM over GrIS while JJA T600 anomaly from GCM and JJA TAS anomaly from RCM compare well. Such discrepancies in the GCM fields can also be seen by comparing anomalies from JJA TAS and JJA T600 simulated by GCM in Fig. 4b, c. Indeed, regarding the JJA TAS increase over 1980–2011 (Fig. 4c), only CanESM2 reproduces the one simulated by ERA-INTERIM but, it is one of the CMIP5 GCMs simulating the highest JJA TAS increase although it is not the case for JJA T600. Similar discrepancies can also be seen for MIROC5 (resp. NorESM1) which overestimates (resp. underestimates) the JJA T600 CMIP5 multi-model mean and underestimates (overestimates) the JJA TAS CMIP5 ensemble mean. This shows that the variability of the RCM-based TAS does not depend on the GCM-based TAS but well on the GCM-based JJA T600 and that using TAS anomaly coming from GCM for evaluating changes over GrIS could be questionable with respect to RCMs using a physically based surface scheme well adapted and validated over GrIS. This highlights the use of RCMs for studying near-surface changes.

Therefore, as suggested above and according to Fettweis et al. (2012), the RCM simulated meltwater run-off anomalies can be estimated using the JJA T600 anomaly from GCM as shown in Fig. 7d. Temperatures at 600 hPa have been chosen to be independent of the surface scheme used in the GCMs and because the JJA T600 well explains the melt variability over current climate (as explained earlier). Figure 7c and d are similar and the same conclusions regarding the meltwater run-off sensitivity to JJA GCM-based T600 or JJA RCM-based TAS increase could be made. Notably, the MARv2-based meltwater run-off sensitivity to a same JJA GCM-based T600 is almost independent (i.e. with differences lower than 100 GT yr^{-1}) of the GCM used as forcing for the CanESM2, MIROC5 and NorESM1-M forced MARv2 simulations. Such an independence in the used forcing occurs because no change in general circulation is projected by the GCMs and therefore, these changes are only driven by the warming of the atmosphere independently of the GCM used as forcing.

Future projections of the Greenland ice sheet surface mass balance

X. Fettweis et al.

[Title Page](#)[Abstract](#)[Introduction](#)[Conclusions](#)[References](#)[Tables](#)[Figures](#)[⏪](#)[⏩](#)[◀](#)[▶](#)[Back](#)[Close](#)[Full Screen / Esc](#)[Printer-friendly Version](#)[Interactive Discussion](#)

6 Future SMB changes based on CMIP5 multi-model mean

6.1 Estimation of SMB from GCM results only

Boosted by the good comparison RCM vs. GCM in Fig. 7d, we can then approximate the MAR-based GrIS SMB anomalies from GCM results only using the following equation:

$$\Delta\text{SMB} \approx \Delta\text{SF} - 84.2 \cdot \Delta T_{600\text{JJA}} - 2.4 \cdot (\Delta T_{600\text{JJA}})^2 - 1.6 \cdot (\Delta T_{600\text{JJA}})^3 \quad (1)$$

where ΔSF is the snowfall anomaly simulated by GCMs over GrIS (see Sect. 5.1) and where the third order polynomial equation in the GCM-based JJA T600 is plotted in black in Fig. 7d. The coefficients of this polynomial equation have been chosen to best fit the $\text{MARv2}_{\text{MIROC5}}$, $\text{MARv2}_{\text{CanESM2}}$ and $\text{MARv2}_{\text{NorESM1-M}}$ results since the other simulations overestimate or underestimate the meltwater run-off anomalies with respect to current climate.

The ability of approximating the RCM-based GrIS SMB using Eq. (1) is shown in Fig. 7e. The RMSE between the GCM-derived SMB and the MARv2-simulated one for the three reference future projections is 87 (resp. 35) GT yr^{-1} while the correlation coefficient is 0.89 (resp. 0.98) without (resp. after) applying a 10 yr running mean to the time series. Such agreement gives us some confidence in our GCM-based SMB estimates using Eq. (1). More detailed statistics for the three reference simulations ($\text{MARv2}_{\text{MIROC5}}$, $\text{MARv2}_{\text{CanESM2}}$ and $\text{MARv2}_{\text{NorESM1-M}}$) can be found in Table S2 in the Supplement. Finally, it should be mentioned that Eq. (1) can only be used to estimate SMB anomalies at the scale of the whole ice sheet and does not work for estimating SMB anomalies at finer spatial scales.

7 Discussion

Although the responses of the MARv2-based meltwater run-off to CanESM2, MIROC5 and NorESM1-M based JJA T600 anomalies is almost identical, these three GCMs project such JJA T600 anomalies at different times. Therefore, we cannot confidently conclude what are the more likely SMB changes for a certain RCP scenario at the end of this century because the differences in the projected SMB can be twice as high. This shows that the main uncertainty in these future projections is related to the GCMs sensitivity to a GHG increase. That is why, since forcing MAR with all CMIP5 GCMs is too time-expensive in computer, it is useful to evaluate what could project MAR if it is forced by other GCMs from the CMIP5 database with the help of Eq. (1). We obviously need to assume that the MAR-based SMB sensitivity to GCM-based anomalies is the same than if MAR is forced by CanESM2, MIROC5 and NorESM1-M. Equation (1) allows also to estimate which of our simulations is the closest to the CMIP5 ensemble mean (noted $30ENS_{CMIP5}$ hereafter) often considered by the IPCC as the most likely future.

According to Fig. 8, the increase of snowfall that is projected by $MARv2_{MIROC5}$ (resp. $MARv2_{CanESM2}$ and $MARv2_{NorESM1-M}$) are below (resp. above) ENS_{CMIP5} . Regarding the projected SMB decreases, $MARv2_{MIROC5}$ is the closest to $30ENS_{CMIP5}$ while $MARv2_{CanESM2}$ (resp. $MARv2_{NorESM1-M}$) overestimates (resp. underestimates) the SMB changes projected by $30ENS_{CMIP5}$. Therefore, notably for the aim of forcing ice sheet models in the framework of the ICE2SEA project, $MARv2_{MIROC5}$ seems to be the best since it compares very well over 1980–1999 with $MARv2_{ERA-INTERIM}$ and its future projections are close to the CMIP5 multi-model mean.

In 2100, $30ENS_{CMIP5}$ projects a sea level rise due to changes in GrIS SMB to be $\sim +4.3 \pm 2.2$ cm and $\sim +8.9 \pm 4.2$ cm for RCP 4.5 and RCP 8.5 experiment, respectively. These projections are in the range of previous estimates (IPCC, 2007).

If we use a SMB anomaly $< -400 \text{ GT yr}^{-1}$ as threshold for having a negative SMB (since the SMB over 1980–1999 is simulated by MAR and RACMO2 to be

Future projections of the Greenland ice sheet surface mass balance

X. Fettweis et al.

Title Page

Abstract

Introduction

Conclusions

References

Tables

Figures



Back

Close

Full Screen / Esc

Printer-friendly Version

Interactive Discussion

$\sim 400 \text{ GT yr}^{-1}$), 30ENS_{CMIP5} suggests that such SMB rates are projected to occur beyond this century according to RCP45 but should occur around 2070 according to the RCP85 scenario. As shown in Fig. 7f, the GrIS SMB anomalies simulated by MARv2 can also be approximated by

$$\begin{aligned} \Delta \text{SMB} \simeq & -71.5 \cdot \Delta \text{TAS}_{\text{global}} \\ & - 20.4 \cdot (\Delta \text{TAS}_{\text{global}})^2 - 2.8 \cdot (\Delta \text{TAS}_{\text{global}})^3 \end{aligned} \quad (2)$$

where TAS ($\text{TAS}_{\text{global}}$) is the annual global TAS anomaly (Eq. 2 is plotted in black in Fig. 7f). This means that a global TAS anomaly of $\sim +3^\circ\text{C}$ is needed for having a SMB anomaly $< -400 \text{ GT yr}^{-1}$ (see also Fig. S6 in the Supplement). By comparison with Eq. (1) based SMB estimations, the RMSE between the global TAS derived SMB and the MARv2-simulated one for the three reference future projections is 137 (resp. 60) GT yr^{-1} while the correlation coefficient is 0.67 (resp. 0.90) without (resp. after) applying a 10 yr running mean to the time series.

In addition to the uncertainties linked to the models/scenarios, it should be noted that these SMB projections do not take into account changes in ice dynamics and surface topography as described in Gregory and Huybrechts (2006). Since the GrIS topography is fixed during our simulations, we neglect the melt/elevation feedback, which could accelerate the melt increase (Helsen et al., 2012). Indeed, prolonged thinning of the ablation zone (as shown in Fig. 9) causes an additional warming for these areas, which should be lower in altitude if the topography could evolve during the simulation. Therefore, our projections are conservative and likely underestimate the GrIS SMB changes.

8 Conclusions

Future projections of the Greenland ice sheet SMB were carried out for the period 2006–2100 for the scenarios RCP 4.5 and RCP 8.5 with the regional climate model MAR forced by the outputs of three GCMs from the CMIP5 database. The GCMs

Future projections of the Greenland ice sheet surface mass balance

X. Fettweis et al.

Title Page

Abstract

Introduction

Conclusions

References

Tables

Figures

⏪

⏩

◀

▶

Back

Close

Full Screen / Esc

Printer-friendly Version

Interactive Discussion



have been chosen for their ability to simulate the current climate (general circulation at 500 hPa and JJA temperature at 700 hPa) over Greenland with respect to the ERA-INTERIM reanalysis. Most of the differences between MAR forced by ERA-INTERIM (which we consider here as the best representation of the current SMB) and forced by CMIP5 GCMs over 1980–1999 are below the discrepancies between MAR forced by ERA-40 and by ERA-INTERIM. Therefore, we can consider MAR forced by these three CMIP5 models (CanESM2, MIROC5 and NorESM1-M) successfully simulates the current SMB over GrIS. However, all simulations fail to model the 2000's substantial decrease of SMB, which might be related to large-scale circulation anomalies rather than a long term change.

In terms of future projections, MAR simulates a substantial decrease of the SMB along the ice sheet margins due to increasing melt and a relatively smaller SMB increase in the interior of the ice sheet due to heavier snowfall. At the scale of the whole ice sheet, the increase of precipitation does not compensate the increase of run-off and MAR simulates a mean surface mass loss of about $\sim 200\text{--}400$ (resp. $\sim 600\text{--}1200$) GT yr^{-1} over 2080–2099 for the RCP 4.5 (resp. RCP 8.5) scenario with respect to the current climate (1980–1999). The large range in this MAR-based future projections is due to the sensitivity of the used GCMs to a same GHG forcing. This indicates that the main uncertainty in our study comes from the GCMs and, RCMs with realistic melt physics and high horizontal resolution remain vital for assessing current climate and SMB and future changes.

However, we can highlight in these future projections that:

1. Heavier winter accumulation dampens the melt increase at the end of spring which explains why no significant increase of the melting season length is projected.
2. Surface melt increases non-linearly with warmer climates because of the expansion of bare ice zones in summer, which decreases the ice sheet meltwater re-freezing capacity and enhances the positive melt/surface albedo feedback. In

Future projections of the Greenland ice sheet surface mass balance

X. Fettweis et al.

Title Page

Abstract

Introduction

Conclusions

References

Tables

Figures



Back

Close

Full Screen / Esc

Printer-friendly Version

Interactive Discussion



Future projections of the Greenland ice sheet surface mass balance

X. Fettweis et al.

Title Page	
Abstract	Introduction
Conclusions	References
Tables	Figures
◀	▶
◀	▶
Back	Close
Full Screen / Esc	
Printer-friendly Version	
Interactive Discussion	

Discussion Paper | Discussion Paper | Discussion Paper | Discussion Paper | Discussion Paper

addition, since most of the precipitation should fall as rainfall instead of snowfall in summer, this contributes to accelerate the melt. Finally, meltwater run-off sensitivity to warmer climates depends on the GCM ability to simulate the current climate and notably the summer atmospheric temperatures. Indeed, if the GCM is too warm over current climate, the impact of a warmer climate is amplified since the response of melt to rising temperatures is not linear due to the positive albedo feedback. This indicates that it is important to well simulate the current climate before making future projections.

3. The SMB decrease simulated by MAR can be estimated using snowfall and JJA 600 hPa temperature anomalies from the forcing GCMs since no GCM projects general circulation changes.

The GCM-based SMB estimates considered here were used to estimate the eustatic sea level rise from the CMIP5 multi-model mean (30 GCMs were used). For RCP4.5 (resp. RCP8.5), the ensemble mean projects a cumulated sea level rise of about $\sim +4 \pm 2$ cm (resp. $\sim +9 \pm 4$). It is important to note that these projections of sea level rise from Greenland ice sheet mass loss do not take into account changes in ice dynamics and in surface topography which could amplify the deglaciation of Greenland due to the positive melt/elevation feedback. Our projections are assumed to be conservative and likely underestimate the SMB decreases.

At the end of this century, according to the RCP8.5 scenario, cumulated anomalies of surface height due to SMB decrease could reach 100–200 m in some areas along the ice sheet margin, emphasizing the necessity of taking into account changes in topography. That is why, it is needed to couple RCMs like MAR and RACMO2 with an ice sheet model to evaluate the feedbacks between surface thinning ice sheet area decline and changes to the SMB (Helsen et al., 2012). Moreover, this coupling will allow to evaluate changes in total Greenland ice sheet mass balance and so to evaluate the sea level rise coming from all changes of mass of the ice sheet.



Supplementary material related to this article is available online at:
<http://www.the-cryosphere-discuss.net/6/3101/2012/tcd-6-3101-2012-supplement.pdf>.

Acknowledgements. Xavier Fettweis is a postdoctoral researcher of the Belgian National Fund for Scientific Research. For their roles in producing, coordinating, and making available the CMIP5 model output, we acknowledge the climate modelling groups (listed in Table 1 of this paper), the World Climate Research Programme's (WCRP) Working Group on Coupled Modelling (WGCM), and the Global Organization for Earth System Science Portals (GO-ESSP). We thank Jamie Rae for having provided the ECHAM5 and HadCM3 outputs and Jonathan Gregory for his helpful comments. Finally, this work was partly supported by funding from the ICE2SEA programme from the European Union 7th Framework Programme (FP7), grant number 226375 (ice2sea contribution number 098). Marco Tedesco's work was supported by the NSF grant # ARC0909388.

References

- Bamber, J. L., Layberry, R. L., and Gogenini, S. P.: A new ice thickness and bed data set for the Greenland ice sheet 1: measurement, data reduction, and errors, *J. Geophys. Res.*, 106, 33773–33780, 2001. 3106
- Belleflamme, A., Fettweis, X., Lang, C., and Erpicum, M.: Current and future atmospheric circulation at 500 hPa over Greenland simulated by the CMIP3 and CMIP5 global models, *Clim. Dynam.*, submitted, 2012. 3110, 3115, 3116
- Bengtsson, L., Koumoutsaris, S., and Hodges, K.: Large-scale surface mass balance of ice sheets from a comprehensive atmospheric model, *Surv. Geophys.*, 32, 459–474, 2011. 3104
- Box, J. E., Bromwich, D. H., and Bai, L.-S.: Greenland ice sheet surface mass balance for 1991–2000: application of Polar MM5 mesoscale model and in-situ data, *J. Geophys. Res.*, 109, D16105, doi:10.1029/2003JD004451, 2004. 3103, 3122
- Box, J. E., Fettweis, X., Stroeve, J. C., Tedesco, M., Hall, D. K., and Steffen, K.: Greenland ice sheet albedo feedback: thermodynamics and atmospheric drivers, *The Cryosphere Discuss.*, 6, 593–634, doi:10.5194/tcd-6-593-2012, 2012. 3107, 3115, 3120

Future projections of the Greenland ice sheet surface mass balance

X. Fettweis et al.

Title Page

Abstract

Introduction

Conclusions

References

Tables

Figures

◀

▶

◀

▶

Back

Close

Full Screen / Esc

Printer-friendly Version

Interactive Discussion



Discussion Paper | Discussion Paper | Discussion Paper | Discussion Paper | Discussion Paper

- Brun, E., David, P., Sudul, M., and Brunot, G.: A numerical model to simulate snowcover stratigraphy for operational avalanche forecasting, *J. Glaciol.*, 38, 13–22, 1992. 3105
- Dee, D. P., Uppala, S. M., Simmons, A. J., Berrisford, P., Poli, P., Kobayashi, S., Andrae, U., Balmaseda, M. A., Balsamo, G., Bauer, P., Bechtold, P., Beljaars, A. C. M., van de Berg, L., Bidlot, J., Bormann, N., Delsol, C., Dragani, R., Fuentes, M., Geer, A. J., Haimberger, L., Healy, S. B., Hersbach, H., Hólm, E. V., Isaksen, L., Kållberg, P., Köhler, M., Matricardi, M., McNally, A. P., Monge-Sanz, B. M., Morcrette, J.-J., Park, B.-K., Peubey, C., de Rosnay, P., Tavolato, C., Thépaut, J.-N., and Vitart, F.: The ERA-Interim reanalysis: configuration and performance of the data assimilation system, *Quart. J. R. Meteorol. Soc.*, 137, 553–597, 2011. 3111
- Deser, C., Tomas, R., Alexander, M., and Lawrence, D.: The seasonal atmospheric response to projected Arctic Sea ice loss in the late twenty-first century, *J. Climate*, 23, 333–351, doi:10.1175/2009JCLI3053.1, 2010. 3119
- Fettweis, X.: Reconstruction of the 1979–2006 Greenland ice sheet surface mass balance using the regional climate model MAR, *The Cryosphere*, 1, 21–40, doi:10.5194/tc-1-21-2007, 2007. 3104
- Fettweis, X., Gallée, H., Lefebvre, L., and van Ypersele, J.-P.: Greenland surface mass balance simulated by a regional climate model and comparison with satellite derived data in 1990–1991, *Clim. Dynam.*, 24, 623–640, doi:10.1007/s00382-005-0010-y, 2005. 3104, 3106, 3107
- Fettweis, X., Gallée, H., Lefebvre, L., and van Ypersele, J.-P.: The 1988–2003 Greenland ice sheet melt extent by passive microwave satellite data and a regional climate model, *Clim. Dynam.*, 27, 531–541, doi:10.1007/s00382-006-0150-8, 2006. 3107
- Fettweis, X., Hanna, E., Gallée, H., Huybrechts, P., and Ericum, M.: Estimation of the Greenland ice sheet surface mass balance for the 20th and 21st centuries, *The Cryosphere*, 2, 117–129, doi:10.5194/tc-2-117-2008, 2008. 3103, 3104, 3122
- Fettweis, X., Mabilille, G., Ericum, M., Nicolay, S., and van den Broeke, M.: The 1958–2009 Greenland ice sheet surface melt and the mid-tropospheric atmospheric circulation, *Clim. Dynam.*, 36, 139–159, doi:10.1007/s00382-010-0772-8, 2011a. 3109, 3113, 3115
- Fettweis, X., Tedesco, M., van den Broeke, M., and Ettema, J.: Melting trends over the Greenland ice sheet (1958–2009) from spaceborne microwave data and regional climate models, *The Cryosphere*, 5, 359–375, doi:10.5194/tc-5-359-2011, 2011b. 3104, 3106, 3107
- Fettweis, X., Belleflamme, A., Ericum, M., Franco, B., and Nicolay, S.: Estimation of the Sea Level Rise by 2100 Resulting from Changes in the Surface Mass Balance of the Greenland

Future projections of the Greenland ice sheet surface mass balance

X. Fettweis et al.

[Title Page](#)[Abstract](#)[Introduction](#)[Conclusions](#)[References](#)[Tables](#)[Figures](#)[⏪](#)[⏩](#)[◀](#)[▶](#)[Back](#)[Close](#)[Full Screen / Esc](#)[Printer-friendly Version](#)[Interactive Discussion](#)

Future projections of the Greenland ice sheet surface mass balance

X. Fettweis et al.

Title Page

Abstract

Introduction

Conclusions

References

Tables

Figures

◀

▶

◀

▶

Back

Close

Full Screen / Esc

Printer-friendly Version

Interactive Discussion



Ice Sheet, Climate Change – Geophysical Foundations and Ecological Effects, edited by: Blanco, J. and Kheradmand, H., ISBN: 978-953-307-419-1, InTech, 2011c. 3111, 3122

Fettweis, X., Hanna, E., Lang, C., Belleflamme, A., Erpicum, M., and Gallé, H.: Important role of the mid-tropospheric atmospheric circulation in the recent surface melt increase over the Greenland ice sheet, *The Cryosphere*, submitted, 2012. 3109, 3114, 3115, 3124

Franco, B., Fettweis, X., Erpicum, M., and Nicolay, S.: Present and future climates of the Greenland ice sheet according to the IPCC AR4 models, *Clim. Dynam.*, Vol. 36, 1897–1918, doi:10.1007/s00382-010-0779-1, 2011. 3104, 3116, 3118

Franco, B., Fettweis, X., Lang, C., and Erpicum, M.: Impact of spatial resolution on the modelling of the Greenland ice sheet surface mass balance between 1990–2010, using the regional climate model MAR, *The Cryosphere*, 6, 695–711, doi:10.5194/tc-6-695-2012, 2012a. 3104, 3106, 3107

Franco, B., Fettweis, X., and Erpicum, M.: Future projections of the Greenland ice sheet energy balance driving the surface melt, developed using the regional climate MAR model, *The Cryosphere Discuss.*, 6, 2265–2303, doi:10.5194/tcd-6-2265-2012, 2012b. 3119, 3120, 3122

Gallée, H. and Schayes, G.: Development of a three-dimensional meso- γ primitive equations model, *Mon. Weather Rev.*, 122, 671–685, 1994. 3105

Gallée, H., Guyomarc'h, G., and Brun, E.: Impact of the snow drift on the Antarctic ice sheet surface mass balance: possible sensitivity to snow-surface properties, *Bound.-Lay. Meteorol.*, 99, 1–19, 2001. 3105

Graversen R., Drijfhout, S., Hazeleger, W., van de Wal, R., Bintanja, R., and Helsen H.: Greenland's contribution to global sea-level rise by the end of the 21st century, *Clim. Dynam.*, 37, 1427–1442, 2010.

Gregory, J. and Huybrechts, P.: Ice-sheet contributions to future sea-level change, *Philos. T. R. Soc. A*, 364, 1709–1731, 2006. 3103, 3104, 3121, 3127

Hanna, E., Cappelen, J., Fettweis, X., Huybrechts, P., Luckman, A., and Ribergaard, M. H.: Hydrologic response of the Greenland ice sheet: the role of oceanographic warming, *Hydrol. Process.*, 23, 7–30, 2009. 3110

Hanna, E., Jones, J. M., Cappelen, J., Mernild, S. H., Wood, L., Steffen, K., and Huybrechts, P.: The influence of North Atlantic atmospheric and oceanic forcing effects on 1900–2010 Greenland summer climate and ice melt/runoff, *Int. J. Climatol.*, doi:10.1002/joc.3475, 2012. 3115

Future projections of the Greenland ice sheet surface mass balance

X. Fettweis et al.

Title Page

Abstract

Introduction

Conclusions

References

Tables

Figures

◀

▶

◀

▶

Back

Close

Full Screen / Esc

Printer-friendly Version

Interactive Discussion

- Helsen, M. M., van de Wal, R. S. W., van den Broeke, M. R., van de Berg, W. J., and Oerlemans, J.: Coupling of climate models and ice sheet models by surface mass balance gradients: application to the Greenland Ice Sheet, *The Cryosphere*, 6, 255–272, doi:10.5194/tc-6-255-2012, 2012. 3127, 3129
- 5 IPCC: Climate Change 2007: The Physical Science Basis. Contribution of Working Group I to the Fourth Assessment Report of the Intergovernmental Panel on Climate Change, edited by: Solomon, S., Qin, D., Manning, M., Chen, Z., Marquis, M., Averyt, K. B., Tignor, M., and Miller, H. L., Cambridge University Press, Cambridge, UK and New York, NY, USA, 2007. 3103, 3104, 3108, 3126
- 10 Lefebre, F., Gallée, H., van Ypersele, J., and Greuell, W.: Modeling of snow and ice melt at ETH-camp (West Greenland): a study of surface albedo, *J. Geophys. Res.*, 108, 4231, doi:10.1029/2001JD001160, 2003. 3104, 3107
- Lefebre, F., Fettweis, X., Gallée, H., van Ypersele, J., Marbaix, P., Greuell, W., and Calanca, P.: Evaluation of a high-resolution regional climate simulation over Greenland, *Clim. Dynam.*, 25, 99–116, doi:10.1007/s00382-005-0005-8, 2005. 3104, 3107
- 15 Lenaerts, J. T. M., van den Broeke, M. R., van Angelen, J. H., van Meijgaard, E., and Déry, S. J.: Drifting snow climate of the Greenland ice sheet: a study with a regional climate model, *The Cryosphere Discuss.*, 6, 1611–1635, doi:10.5194/tcd-6-1611-2012, 2012. 3103, 3107
- Mernild, S. H., Liston, G. E., and Hasholt, B.: East Greenland freshwater run-off to the Greenland-Iceland-Norwegian Seas 1999–2004 and 2071–2100, *Hydrol. Process.*, 22, 4571–4586, 2008. 3104
- 20 Mernild, S. H., Liston, G. E., Hiemstra, C. A., and Christensen, J. H.: Greenland ice sheet surface mass-balance modeling in a 131-yr perspective, 1950–2080, *J. Hydrometeorol.*, 11, 3–25, doi:10.1175/2009JHM1140.1, 2010. 3104, 3118
- 25 Mernild, S. H., Knudsen, N. T., Lipscomb, W. H., Yde, J. C., Malmros, J. K., Hasholt, B., and Jakobsen, B. H.: Increasing mass loss from Greenland's Mittivakkat Gletscher, *The Cryosphere*, 5, 341–348, doi:10.5194/tc-5-341-2011, 2011.
- Moss, R. H., Edmonds, J. A., Hibbard, K., Manning, M., Rose, S. K., van Vuuren, D. P., Carter, T. R., Emori, S., Kainuma, M., Kram, T., Meehl, G., Mitchell, J., Nakicenovic, N., Riahi, K., Smith, S., Stouffer, R. J., Thomson, A., Weyant, J., and Wilbanks, T.: The next generation of scenarios for climate change research and assessment, *Nature*, 463, 747–756, doi:10.1038/nature08823, 2010. 3107
- 30

Future projections of the Greenland ice sheet surface mass balance

X. Fettweis et al.

Title Page

Abstract

Introduction

Conclusions

References

Tables

Figures

◀

▶

◀

▶

Back

Close

Full Screen / Esc

Printer-friendly Version

Interactive Discussion



- Mote, T. L.: Estimation of runoff rates, mass balance, and elevation changes on the Greenland ice sheet from passive microwave observations, *J. Geophys. Res.*, 108, 4056, doi:10.1029/2001JD002032, 2003. 3112, 3123
- Nick, F. M., Vieli, A., Howat, I. M., and Joughin, I.: Large-scale changes in Greenland outlet glacier dynamics triggered at the terminus, *Nature Geosci.*, 2, 110–114, doi:10.1038/ngeo394, 2009. 3103
- Picard, G., Domine, F., Krinner, G., Arnaud, L., and Lefebvre, E.: Inhibition of the positive snow-albedo feedback by precipitation in interior Antarctica, *Nature Clim. Change*, doi:10.1038/nclimate1590, 2012. 3120
- Rae, J. G. L., Aðalgeirsdóttir, G., Edwards, T. L., Fettweis, X., Gregory, J. M., Hewitt, H. T., Lowe, J. A., Lucas-Picher, P., Mottram, R. H., Payne, A. J., Ridley, J. K., Shannon, S. R., van de Berg, W. J., van de Wal, R. S. W., and van den Broeke, M. R.: Greenland ice sheet surface mass balance: evaluating simulations and making projections with regional climate models, *The Cryosphere Discuss.*, 6, 2059–2113, doi:10.5194/tcd-6-2059-2012, 2012. 3103, 3104, 3106, 3107, 3123
- Rignot, E., Velicogna, I., van den Broeke, M. R., Monaghan, A., and Lenaerts, J.: Acceleration of the contribution of the Greenland and Antarctic ice sheets to sea level rise, *Geophys. Res. Lett.*, 38, L05503, doi:10.1029/2011GL046583, 2011. 3103, 3115
- Schuenemann, K. C. and Cassano, J. J.: Changes in synoptic weather patterns and Greenland precipitation in the 20th and 21st centuries: 2. Analysis of 21st century atmospheric changes using self-organizing maps, *J. Geophys. Res.*, 115, D05108, doi:10.1029/2009JD011706, 2010. 3122
- Screen, J. A. and Simmonds, I.: Erroneous Arctic temperature trends in the ERA-40 reanalysis: a closer look, *J. Climate*, 24, 2620–2627, doi:10.1175/2010JCLI4054.1, 2011. 3111
- Serreze, M. C., Barrett, A. P., Stroeve, J. C., Kindig, D. N., and Holland, M. M.: The emergence of surface-based Arctic amplification, *The Cryosphere*, 3, 11–19, doi:10.5194/tc-3-11-2009, 2009. 3114
- Sundal, A. V., Shepherd, A., Nienow, P., Hanna, E., Palmer, S., and Huybrechts, P.: Melt-induced speed-up of Greenland ice sheet offset by efficient subglacial drainage, *Nature*, 469, 521–524, doi:10.1038/nature09740, 2011. 3103
- Swingedouw, D., Mignot, J., Braconnot, P., Mosquet, E., Kageyama, M. and Alkama, R.: Impact of freshwater release in the North Atlantic under different climate conditions in an OAGCM, *J. Climate*, 22, 6377–6403, 2009. 3104

Future projections of the Greenland ice sheet surface mass balance

X. Fettweis et al.

Title Page

Abstract

Introduction

Conclusions

References

Tables

Figures

◀

▶

◀

▶

Back

Close

Full Screen / Esc

Printer-friendly Version

Interactive Discussion



Table 1. Summary of the different forcings and scenarios used in the MAR simulations.

Boundaries RCM forcing	Institutes, Country	Period	Scenario
ERA-40 reanalysis	ECMWF, UK	1957–2001	
ERA-INTERIM reanalysis	ECMWF, UK	1979–2011	
BCC-CSM1-1 (CMIP5)	Beijing Climate Center, China	1975–1999	Historical
BCC-CSM1-1 (CMIP5)	Beijing Climate Center, China	2075–2099	RCP85
CanESM2 (CMIP5)	Canadian Centre for Climate Modelling and Analysis, Canada	1965–2005	Historical
CanESM2 (CMIP5)	Canadian Centre for Climate Modelling and Analysis, Canada	2006–2100	RCP45 and RCP85
ECHAM5 (ICE2SEA)	Max Planck Institute for Meteorology, Germany	1980–1999	SRES 20C3M
ECHAM5 (ICE2SEA)	Max Planck Institute for Meteorology, Germany	2000–2099	SRES A1B
HadCM3 (ICE2SEA)	Met Office Hadley Centre, UK	1980–1999	SRES 20C3M
HadCM3 (ICE2SEA)	Met Office Hadley Centre, UK	2000–2099	SRES A1B
MIROC5 (CMIP5)	The University of Tokyo, Japan	1965–2005	Historical
MIROC5 (CMIP5)	The University of Tokyo, Japan	2006–2100	RCP45 and RCP85
NorESM1-M (CMIP5)	Norwegian Climate Centre, Norway	1965–2005	Historical
NorESM1-M (CMIP5)	Norwegian Climate Centre, Norway	2006–2100	RCP26, RCP45, RCP60 and RCP85

Future projections of the Greenland ice sheet surface mass balance

X. Fettweis et al.

Table 2. Average and standard deviation of the annual surface mass balance components simulated by MAR and RACMO2 over 1980–1999. Units are GT yr^{-1} and acronym of each simulation ($\text{RCM}_{\text{forcings}}$) is given in the first column. The surface mass balance (SMB) equation is here $\text{SMB} = \text{snowfall} + \text{rainfall} - \text{run-off} - \text{water fluxes}$. The run-off is the part of not re-frozen water from both surface melt and rainfall reaching the ocean. Finally, the blowing snow sublimation is (resp. not) taken into account in the RACMO2 (resp. MAR) simulations.

Simulation acronym	SMB	Snowfall	Rainfall	Run-off	Water fluxes	Meltwater
MARv2 _{ERA-INTERIM}	388 ± 103	637 ± 55	25 ± 4	266 ± 66	8 ± 2	449 ± 91
MARv1 _{ERA-40}	423 ± 104	635 ± 55	25 ± 4	232 ± 66	5 ± 1	409 ± 95
MARv2 _{ERA-40}	447 ± 106	673 ± 57	28 ± 5	247 ± 68	7 ± 1	429 ± 96
MARv2 _{BCC-CSM1-1}	433 ± 92	585 ± 70	19 ± 7	161 ± 49	9 ± 2	293 ± 66
MARv2 _{CanESM2}	410 ± 102	635 ± 51	37 ± 9	257 ± 84	5 ± 2	414 ± 112
MARv2 _{MIROC5}	437 ± 107	681 ± 65	26 ± 6	266 ± 79	5 ± 2	445 ± 99
MARv2 _{NorESM1-M}	483 ± 71	691 ± 58	28 ± 4	230 ± 42	6 ± 1	401 ± 62
MARv1 _{ECHAM5}	207 ± 88	501 ± 34	24 ± 7	314 ± 80	4 ± 2	488 ± 110
MARv1 _{HadCM3}	114 ± 103	488 ± 49	30 ± 10	397 ± 95	7 ± 2	590 ± 122
RACMO2 _{ERA-40}	406 ± 98	683 ± 60	46 ± 9	282 ± 62	41 ± 4	476 ± 91
RACMO2 _{HadGEM2-ES}	244 ± 110	660 ± 93	54 ± 16	429 ± 98	42 ± 4	657 ± 131

[Title Page](#)
[Abstract](#)
[Introduction](#)
[Conclusions](#)
[References](#)
[Tables](#)
[Figures](#)
[Back](#)
[Close](#)
[Full Screen / Esc](#)
[Printer-friendly Version](#)
[Interactive Discussion](#)


Future projections of the Greenland ice sheet surface mass balance

X. Fettweis et al.

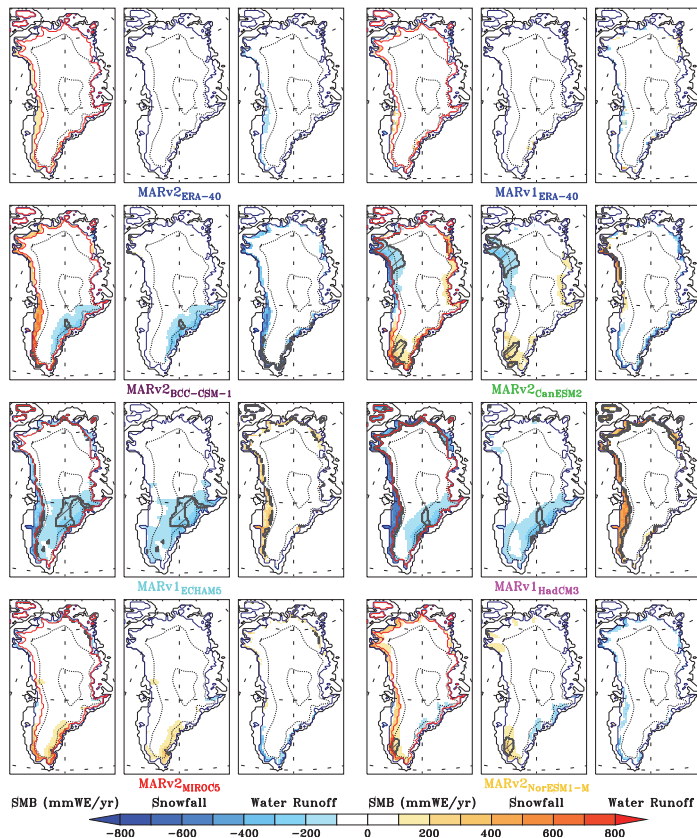


Fig. 1. Mean anomalies over 1980–1999 of the annual SMB, snowfall and water run-off with respect to the ERA-INTERIM-forced MARv2 simulation for the MAR simulations listed in Table 2. Units are mm WE yr^{-1} . The areas where the anomalies are two times above the 1980–1999 standard deviation of MARv2_{ERA-INTERIM} are hatched in dark grey. The ELA from MARv2_{ERA-INTERIM} is plotted in red. Finally, the same comparison with respect to MARv2_{ERA-40} over 1970–1999 is available in the Supplement as Fig. S2.

Title Page

Abstract

Introduction

Conclusions

References

Tables

Figures

◀

▶

◀

▶

Back

Close

Full Screen / Esc

Printer-friendly Version

Interactive Discussion

Future projections of the Greenland ice sheet surface mass balance

X. Fettweis et al.

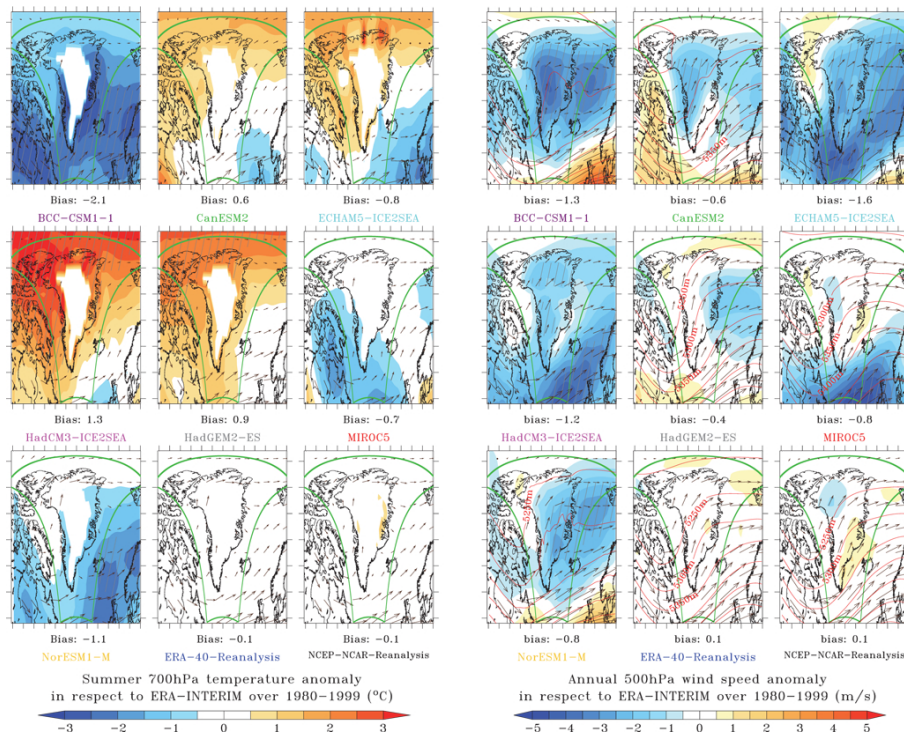


Fig. 2. (Left) Mean anomalies of the JJA 700 hPa Temperature simulated by the different GCMs used in this study with respect to ERA-INTERIM over 1980–1999. The JJA mean wind vectors (not anomalies) at 700 hPa are also plotted and the mean temperature bias is listed in normalised value. Finally, the boundaries of the MAR integration domain are plotted in green and the areas where the anomalies are two times above the 1980–1999 standard deviation of ERA-INTERIM are hatched in dark grey. (Right) Same as (left) but for the annual mean wind speed at 500 hPa. Again, the annual mean wind vectors at 500 hPa are also plotted.

Title Page

Abstract Introduction

Conclusions References

Tables Figures

◀ ▶

◀ ▶

Back Close

Full Screen / Esc

Printer-friendly Version

Interactive Discussion



Future projections of the Greenland ice sheet surface mass balance

X. Fettweis et al.

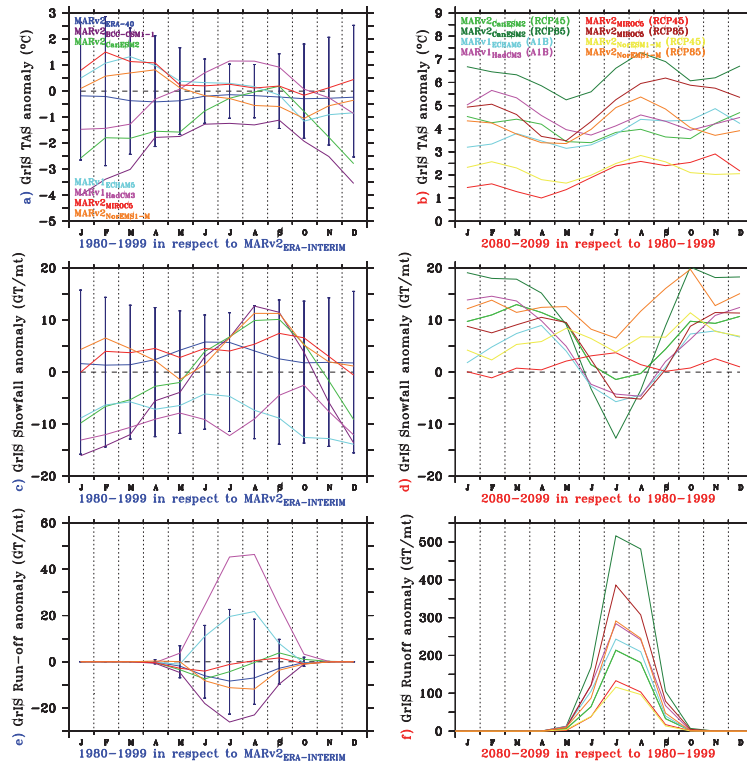


Fig. 3. (a) Monthly anomalies of the GrIS TAS (in °C) simulated by MAR forced by the different listed GCMs with respect to MARv2_{ERA-INTERIM} over 1980–1999. The error bars show the standard deviation of the MARv2_{ERA-INTERIM} simulation over 1980–1999. (b) Same as (a) for the GrIS TAS anomalies over 2080–2099 with respect to MAR forced by the same GCM over 1980–1999. (c) Same as (a) but for the GrIS monthly cumulated snowfall in GT/month. (d) Same as (b) but for the snowfall. (e) Same as (a) but for the GrIS monthly cumulated water run-off in GT/month. (f) Same as (b) but for the water run-off. Finally, a 3-month running mean is applied on each time series for smoothing the curves except in Fig. 3f.

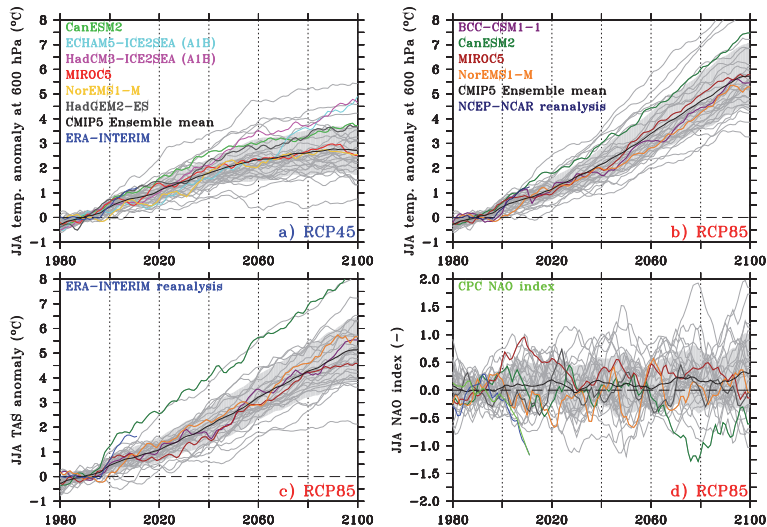


Fig. 4. (a) Anomaly of JJA temperature at 600 hPa (T600) simulated by the reanalyses and the CMIP5 GCMs with respect to 1980–1999 over Greenland for the RCP 4.5 scenario. The anomaly of T600 is taken over an area covering Greenland ($70^{\circ} \text{W} \leq \text{longitude} \leq 20^{\circ} \text{W}$ and $60^{\circ} \text{N} \leq \text{latitude} \leq 85^{\circ} \text{N}$). The ensemble mean as well as the standard deviation of the 30 CMIP5 GCMs are plotted in dark black and in light grey, respectively. Finally, the projections from GCMs used in this study are drawn in colour and a 10-yr running mean is applied for smoothing the curves. (b) Same as (a) but for RCP 8.5. (c) Same as (b) but for JJA TAS over GrIS. In lack of an ice sheet mask in the GCMs, the pixels located in the area described above and at an altitude higher than 1000 meters a.s.l are used for computing the JJA TAS over GrIS. The topography (OROG) of each model is used for selecting the pixels higher than 1000 m a.s.l. (d) Same as (b) but for a proxy of the JJA NAO index. The NAO index is here estimated as the standardized (over 1980–1999) difference of the JJA air pressure at sea level (PSL) between the Azores (27°W , 39°N) and the Iceland (22°W , 64°N). The “real” JJA NAO index from the Climate Prediction Center (CPC) (<http://www.cpc.ncep.noaa.gov/>) is plotted in light green as a comparison. It is also normalised over 1980–1999.

Future projections of the Greenland ice sheet surface mass balance

X. Fettweis et al.

Title Page

Abstract

Introduction

Conclusions

References

Tables

Figures

◀

▶

◀

▶

Back

Close

Full Screen / Esc

Printer-friendly Version

Interactive Discussion

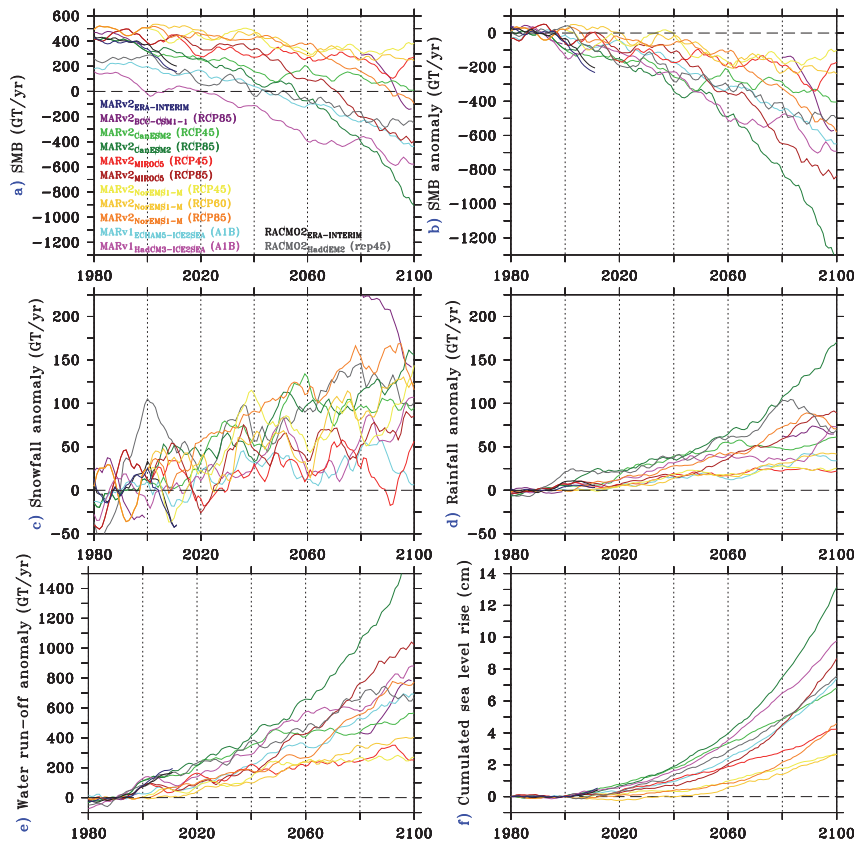


Fig. 5. (a) Time series of the annual total ice sheet SMB (in GT yr^{-1}) simulated by MAR and RACMO2 forced by the listed GCMs over 1980–1999. (b) Same as (a) but for the SMB anomaly with respect to 1980–1999. (c) Same as (b) but for the snowfall. (d) Same as (b) but for the rainfall. (e) Same as (b) but for the JJA near-surface temperature averaged over the GrIS. (f) The corresponding cumulated sea level rise (in cm) from SMB changes. The computations use an ocean area of 361 million km^2 .

Future projections of the Greenland ice sheet surface mass balance

X. Fettweis et al.

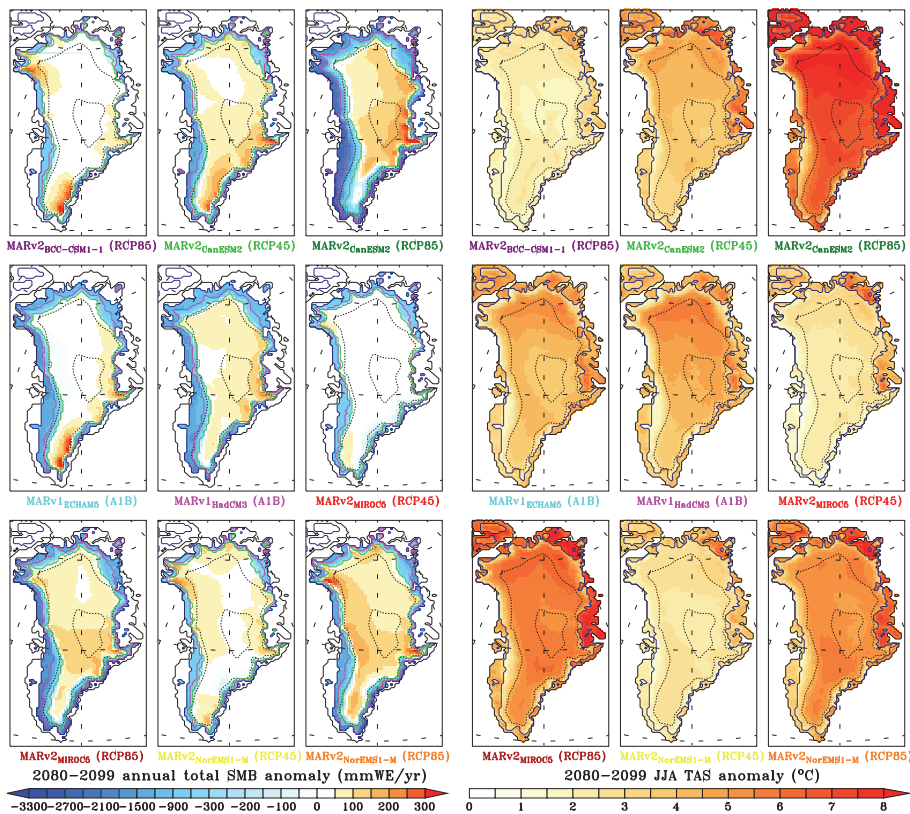


Fig. 6. Anomalies of the mean annual SMB over 2080–2099 with respect to 1980–1999. Units are mmWE yr^{-1} . Finally, the ELA over 1980–1999 (resp. 2080–2099) is plotted in mauve (resp. green).

Title Page

Abstract Introduction

Conclusions References

Tables Figures

◀ ▶

◀ ▶

Back Close

Full Screen / Esc

Printer-friendly Version

Interactive Discussion

Future projections of the Greenland ice sheet surface mass balance

X. Fettweis et al.

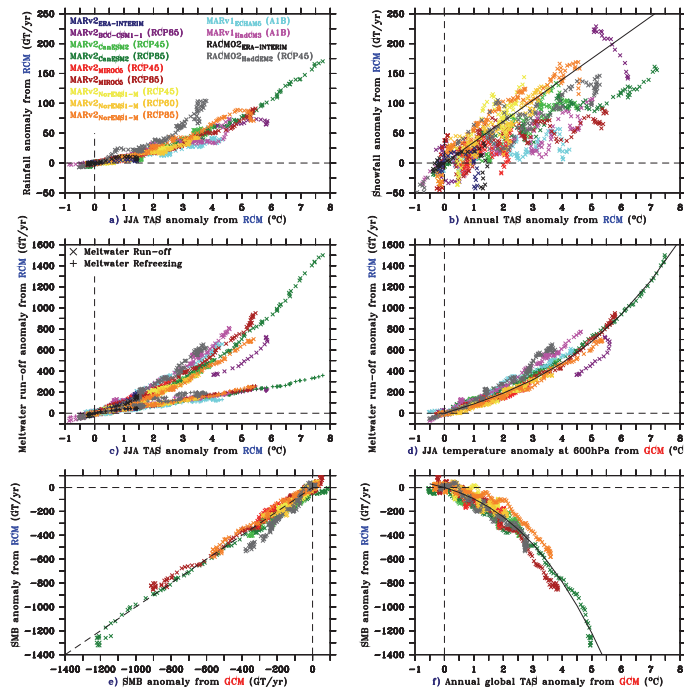


Fig. 7. (a) Anomalies of the annual total GrIS rainfall (in GT yr^{-1}) versus the JJA GrIS TAS anomaly (in $^{\circ}\text{C}$) simulated by the RCMs over 1980–2100. The anomalies are given with respect to 1980–1999 and a 10-yr running mean has been applied to the time series before making the scatter plot. (b) Same as (a) but for annual total snowfall vs annual GrIS TAS. (c) Same as (a) but for annual total meltwater run-off vs JJA GrIS TAS. (d) Same as (a) for annual total meltwater run-off vs the JJAS (from June to September) temperature anomaly from GCM taken at 600 hPa over the area ($70^{\circ}\text{W} \leq \text{longitude} \leq 20^{\circ}\text{W}$ and $60^{\circ}\text{N} \leq \text{latitude} \leq 85^{\circ}\text{N}$). (e) Same as (a) but for the annual total SMB from RCMs vs the estimated one from GCMs using Eq. (1). (f) Same as (a) but for the annual total SMB from RCMs vs the annual global TAS from GCMs.

Title Page

Abstract

Introduction

Conclusions

References

Tables

Figures

◀

▶

◀

▶

Back

Close

Full Screen / Esc

Printer-friendly Version

Interactive Discussion

Future projections of the Greenland ice sheet surface mass balance

X. Fettweis et al.

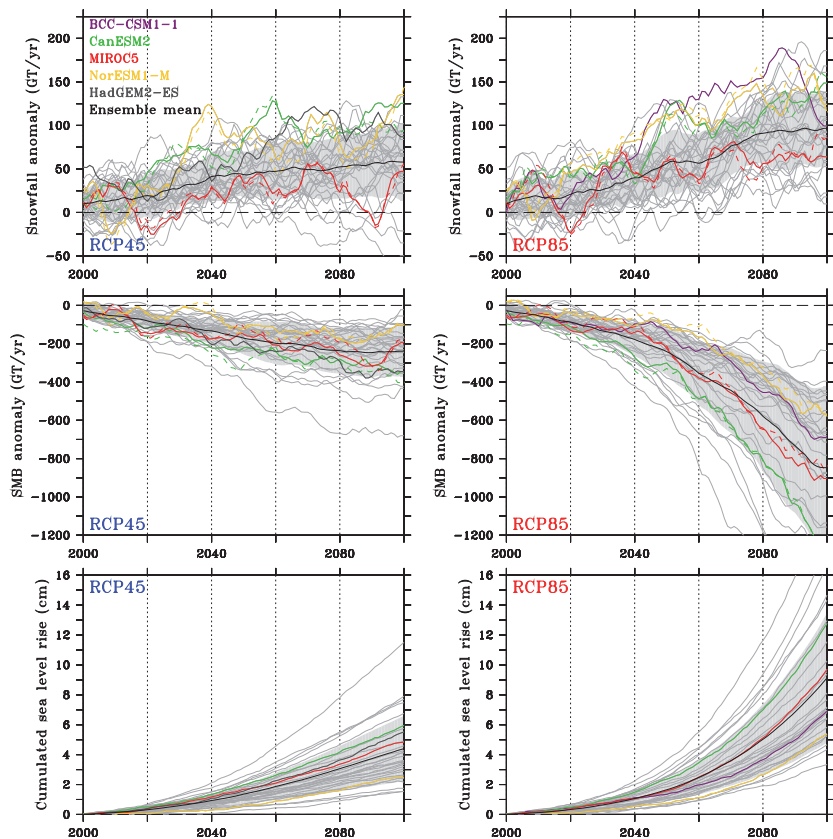


Fig. 8. Same as Fig. 4 but for the GrIS snowfall and SMB anomaly in GT yr^{-1} according to Eq. (1) as well as the corresponding sea level rise in cm. The dashed coloured lines plot the time series from MARv2 forced by the corresponding GCMs.

Title Page

Abstract Introduction

Conclusions References

Tables Figures

◀ ▶

◀ ▶

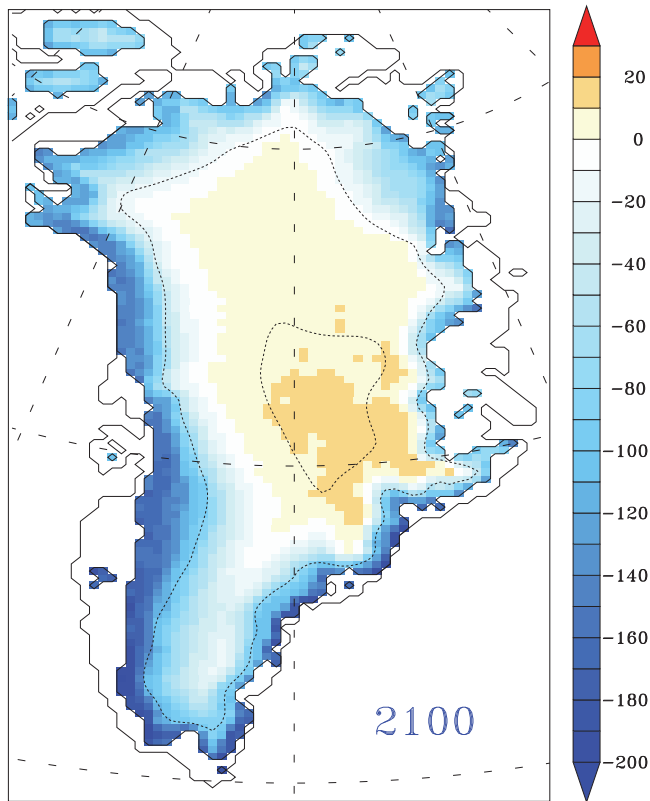
Back Close

Full Screen / Esc

Printer-friendly Version

Interactive Discussion





Cumulated surface height anomaly (in m)

Fig. 9. Cumulated surface height anomaly (in m) from 2000 to 2100 simulated by MARv2_{CanESM2} (RCP85). The anomalies are computed with respect to 1980–1999.

Future projections of the Greenland ice sheet surface mass balance

X. Fettweis et al.

Title Page

Abstract Introduction

Conclusions References

Tables Figures

◀ ▶

◀ ▶

Back Close

Full Screen / Esc

Printer-friendly Version

Interactive Discussion

